5. Hashimoto H, Enjoji M. Liposarcoma: a clinicopathologic subtyping of 52 cases. *Acta Pathol Jpn* 1982;32:933–948
6. Knight JC, Renwick PJ, Cin PD, Van den Berghe H, Fletcher CD. Translocation t(12;16)(q13;p11) in myxoid and round cell liposarcoma: molecular and cytogenetic analysis. *Cancer Res* 1995;55:24–27
7. Panagopoulos I, Mandahl N, Ron D, et al. Characterization of the *CHOP* breakpoints and fusion transcripts in myxoid liposarcomas with the 12;16 translocation. *Cancer Res* 1994;54:6500–6503
8. Kuroda M, Ishida T, Horiuchi H, et al. Chimeric *TLS/FUS-CHOP* gene expression and the heterogeneity of its junction in human myxoid and round cell liposarcoma. *Am J Pathol* 1995;147: 1221–1227
9. Hisaoka M, Tsuji S, Morimitsu Y, et al. Detection of *TLS/FUS-CHOP* fusion transcripts in myxoid and round cell liposarcomas by nested reverse transcription-polymerase chain reaction using archival paraffin-embedded tissues. *Diagn Mol Pathol* 1998;7:96–101
10. Jelinek JS, Kransdorf MJ, Shmookler BM, Aboulafia AJ, Malawer MM. Liposarcoma of the extremities: MR and CT findings in the histologic subtypes. *Radiology* 1993;186:455–459
11. London J, Kim EE, Wallace S, Shirkhoda A, Coan J, Evans H. MR imaging of liposarcomas: correlation of MR features and histology. *J Comput Assist Tomogr* 1989;15:832–835
12. Sundaram M, Baran G, Merenda G, McDonald DJ. Myxoid liposarcoma: MR imaging appearances with clinical and histological correlation. *Skeletal Radiol* 1990;19:359–362
13. Ramsdell MG, Chew FS, Keel SB. Myxoid liposarcoma of the thigh. *AJR* 1998;170:1242
14. Sung MS, Kang HS, Suh JS, et al. Myxoid liposarcoma: appearance at MR imaging with histologic correlation. *RadioGraphics* 2000;20:1007–1019
15. Hasegawa T, Yokoyama R, Lee YH, et al. Prognostic relevance of a histological grading system using MIB-1 for adult soft-tissue sarcoma. *Oncology* 2000;58:66–74
16. Hasegawa T, Yamamoto S, Yokoyama R, et al. Prognostic significance of grading and staging systems using MIB-1 score in adult patients with soft tissue sarcoma of the extremities and trunk. *Cancer* 2002;95:843–851
17. Hasegawa T, Yamamoto S, Nojima T, et al. Validity and reproducibility of histologic diagnosis and grading for adult soft-tissue sarcomas. *Hum Pathol* 2002;33:111–115
18. Kilpatrick SE, Doyon J, Choong PFM, et al. The clinicopathologic spectrum of myxoid and round cell liposarcoma: a study of 95 cases. *Cancer* 1996;77:1450–1458
19. Smith TA, Easley KA, Goldblum JR. Myxoid/round cell liposarcoma of the extremities: a clinicopathologic study of 29 cases with particular attention to extent of round cell liposarcoma. *Am J Surg Pathol* 1996;20:171–180
20. Antonescu CR, Tschernyavsky SJ, Decuseara R, et al. Prognostic impact of p53 status, *TLS-CHOP* fusion transcript structure, and histological grade in myxoid liposarcoma: molecular and clinicopathologic study of 82 cases. *Clin Cancer Res* 2001;7:3977–3987
21. Lack EE, Steinberg SM, White DM, et al. Extremity soft tissue sarcomas: analysis of prognostic variables in 300 cases and evaluation of tumor necrosis as a factor in stratifying high-grade sarcomas. *J Surg Oncol* 1989;41:263–273
22. Mandard AM, Petiot JF, Marnay J, et al. Prognostic factors in soft tissue sarcomas: a multivariate analysis of 109 cases. *Cancer* 1989;63:1437–1451
23. Choong PFM, Gustafson P, Willen H, et al. Prognosis following locally recurrent soft tissue sarcoma: a staging system based on primary and recurrent tumor characteristics. *Int J Cancer* 1995;60:33–37
24. Orson GG, Sim FH, Reiman HM, et al. Liposarcoma of the musculoskeletal system. *Cancer* 1987;60:362–370
25. Reitan JB, Kaazhus O, Brenhoud IO, et al. Prognostic factors in liposarcoma. *Cancer* 1985;55: 2482–2490
26. Arkun R, Memis A, Akalin T, Ustun EE, Sabah D, Kandiloglu G. Liposarcoma of soft tissue: MRI findings with pathologic correlation. *Skeletal Radiol* 1997;26:167–172
27. Munk PL, Lee MJ, Janzen DL, et al. Lipoma and liposarcoma: evaluation using CT and MR imaging. *AJR* 1997;169:589–594
28. Kransdorf MJ. Malignant soft tissue tumors in a large referral population: distribution of diagnoses by age, sex, and location. *AJR* 1995;164: 129–134
29. Kransdorf MJ, Murphey MD. Radiologic evaluation of soft-tissue masses: a current perspective. *AJR* 2000;175:575–587

The reader's attention is directed to the article titled "Lipomas, Lipoma Variants, and Well-Differentiated Liposarcomas (Atypical Lipomas): Results of MRI Evaluations of 126 Consecutive Fatty Masses," which appears on page 733.

Histopathology 2004, 44, 297–306

Correspondence

Gastric glomangiomyoma: a pedunculated extramural mass with a florid angiomyomatous pattern

Sir: Glomus tumours are uncommon mesenchymal tumours with an incidence of about 1.6% among soft tissue tumours. The tumours are most commonly found in the peripheral soft tissues, especially in the distal parts of the extremities.[1] Here, we describe a rare variant of the glomus tumour, glomangiomyoma, in the gastrointestinal tract with an unusual extramural location and a florid smooth muscle cell component.

A 54-year-old Chinese woman presented with recurrent epigastric pain for 2 years. Repeated endoscopies revealed no mucosal lesion but only vague bulging in the posterior wall of the gastric antrum. Computed axial tomography revealed a well-defined, 70-mm paragastric solid mass in the right upper abdomen connected to the stomach by a narrow stalk, extending just inferior to the liver to the level of the aortic bifurcation. The tumour was surgically removed and she has remained well during the last 3 months of follow-up after the operation.

The tumour was a circumscribed ovoid mass weighing 101 g and measuring 70 × 60 × 35 mm with a solid tan-coloured cut surface (Figure 1A). There was no capsule, but the external surface of the tumour was smooth and covered by peritoneum.

Microscopically, the tumour showed a biphasic pattern (Figure 1B). The predominant component was eosinophilic spindle cells whorling around mostly capillary-sized vessels, forming an angiomyoma-like pattern (Figure 1C). These cells were strongly positive for smooth muscle markers including desmin (Figure 1D), smooth muscle actin and muscle-specific actin. The other component was the diagnostic glomus cells, comprising islands and sheets of small ovoid cells surrounding gapped or staghorn-like vessels. These cells possessed well-demarcated round basophilic nuclei and scanty cytoplasm (Figure 1E). Collagen IV and reticulin showed pericellular staining patterns around these cells. Only a few of these cells were positive for desmin (Figure 1F). Both components showed negative staining for AE1/AE3, CD34, C-kit (CD117), S100, HMB45, chromogranin and synaptophysin. Neither necrosis nor cytological atypia were present. The proliferative index of the tumour was low with rare mitotic figures (<1 per 50 high-power fields) and low MIB-2 (Ki67) staining (<1% for both cell components).

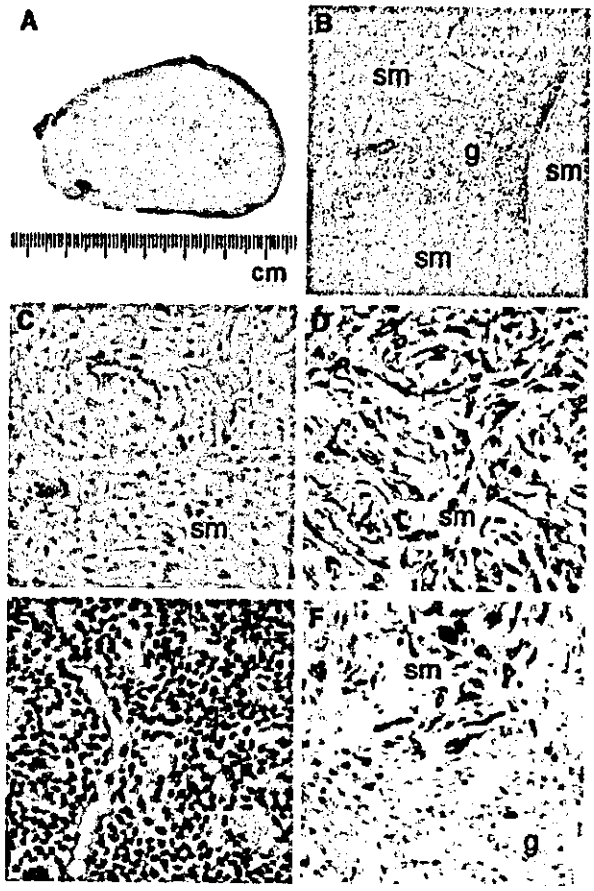

Figure 1. A, Gross appearance of the solid tan-coloured cut surface of the glomangiomyoma. B, Low-power view of H–E section showing a small island of the basophilic ovoid glomus tumour cells (g) surrounded by the abundant smooth muscle cell component (sm). C, High-power view of H–E section showing the whorling pattern of the smooth muscle cells (sm) around vessels. D, Immunostaining of desmin (Dako M760, clone D33, dilution 1 : 150) showing the angiomyomatous pattern of this tumour with the strong staining of the smooth muscle cells (sm). E, High-power view of the H–E section showing the pericytoma-like glomus tumour cell component (g). F, Immunostaining of desmin showing the transition from negatively stained glomus tumour cells (g) to strongly stained smooth muscle cells (sm).

In conclusion, the tumour was a pedunculated, subsersosal gastric glomangiomyoma with a predominant spindled smooth muscle cell component, resulting in a striking angiomyomatous pattern. The tell-tale glomus cell component was only confined to scattered small areas. Glomus tumours have a close growth association with vessels. Variable degrees of differentiation/transformation towards mature smooth muscle cells and a

focal angiomyomatous pattern have previously been described.[1,2] A predominant spindle cell component, as in the present case, however, has not been reported. Accordingly, differential diagnoses include gastrointestinal stromal cell tumour, haemangiopericytoma, solitary fibrous tumour, leiomyoma/leiomyoma of uncertain malignant potential, schwannoma and angiomyolipoma (see Ref. 3 for review).

Miettinen and coworkers[3] reviewed the largest series of 32 gastrointestinal glomus tumours. Most of them were circumscribed, intramural or intraluminal masses located in the gastric antrum. Typically, the presenting symptoms were those of gastrointestinal bleeding or ulcers. Most tumours were small and the patients fared well, except one with a large tumour (65 mm in size), who developed disease metastatic to the liver. The prognostic criteria of gastrointestinal glomangiomyoma or glomus tumours as a whole are not well established. With regard to the large size (70 mm) of the tumour of our patient, long-term follow-up is warranted. For glomus tumour affecting the extremities, location of the tumour in a deeper tissue plane is associated with a poorer prognosis.[4] The depth of primary tumour, however, does not seem to play a significant role in the prognosis for gastrointestinal glomus tumour.[3] Spindle cells in glomus tumours have been suggested to be associated with an adverse prognosis.[3,4] However, it should be noted that among the few unfavourable cases reported, the 'spindle' cells were mostly sarcoma-like, resembling malignant fibrous histiocytoma or leiomyosarcoma.[4] Thus, whether the cytologically bland, spindled smooth muscle component in the present case plays an additional adverse role in the clinical behaviour remains doubtful.

A W I Lo
L T C Chow
K F To
M Y Yu

Department of Anatomical and Cellular Pathology, The Chinese University of Hong Kong, Prince of Wales Hospital, Shatin, New Territories, Hong Kong Special Administration Region, People's Republic of China

1. Weiss SW, Goldblum JR. Perivascular tumors. In Weiss SW, Goldblum JR eds. *Enzinger and Weiss's soft tissue tumours*, 4th edn. St Louis: Mosby, Inc., 2001; 985–1036.
2. Miliauskas JR, Worthley C, Allen PW. Glomangiomyoma (glomus tumour) of the pancreas: a case report. *Pathology* 2002; 34; 193–195.
3. Miettinen M, Paal E, Lasota J, Sobin LH. Gastrointestinal glomus tumours. A clinicopathologic, immunohistochemical, and molecular genetic study of 32 cases. *Am. J. Surg. Pathol.* 2002; 26; 301–311.
4. Folpe AL, Fanburg-Smith JC, Miettinen M, Weiss SW. Atypical and malignant glomus tumors. Analysis of 52 cases, with a proposal for the reclassification of glomus tumors. *Am. J. Surg. Pathol.* 2001; 25; 1–12.

Gastrointestinal zygomycosis: two case reports

Sir: Gastrointestinal zygomycosis is rare. We present one case of small intestinal mucormycosis and one case of colonic and hepatic entomophthoromycosis, documenting the dramatically different clinicopathological features caused by fungi of the two orders of the class *Zygomycetes*.

A 65-year-old Caucasian man with chronic obstructive pulmonary disease admitted with lobar pneumonia rapidly developed respiratory and renal failure. Subsequently, he had a major rectal bleed and emergency extended right hemicolectomy revealed four separate well-demarcated perforations within otherwise normal ileum.

Microscopy showed florid acute inflammation and microabscesses at the perforation sites, associated with abundant multinucleate giant cells (Figure 1). Within the luminal necrotic debris and multinucleate giant cells were abundant irregularly shaped, non-septate hyphae, branching at right angles, morphologically consistent with *Mucorales*. Post-operatively, he was treated with 4 weeks of intravenous amphotericin B. Two years later, he is alive and well.

The second case was a 45-year-old Iranian farmer admitted with right iliac fossa pain. Computed tomography and subsequent right hemicolectomy revealed a 90-mm solid caecal mass which histologically was a caecal abscess containing a striking number of eosinophils, multinucleated giant cells and multiple broad and sparsely septate fungal hyphae surrounded by characteristic 'Splendore–Hoeppli' precipitates (Figure 2). Six weeks later he developed multiple liver abscesses and fine needle aspiration again showed *Entomophthorales* hyphae surrounded by 'Splendore–Hoeppli' precipitates. Treatment with ketaconazole, together with cotrimoxazole, was successful and he was discharged 4 weeks later.

Mucorales and *Entomophthorales*, the two orders of the class *Zygomycetes*, are closely related fungi but have dramatically different disease manifestations.[1] *Mucorales* are opportunistic fungi that cause rapidly disseminating, acute fulminating and often fatal infections in diabetic, debilitated or immunocompromised hosts.[2] Fungi tend to invade blood vessels causing

Figure 1. Small-bowel mucormycosis. Microabscesses and multinucleate giant cells containing *Mucorales* (inset).

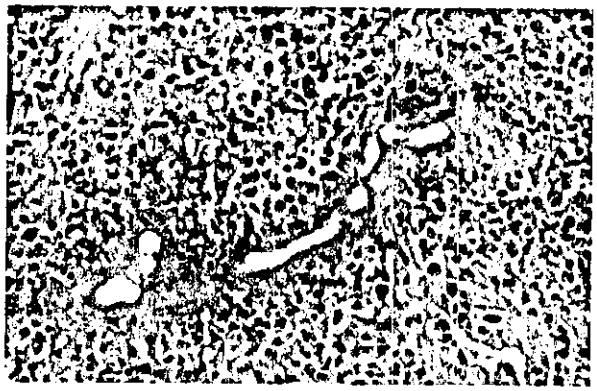

Figure 2. 'Splendore–Hoeppli' precipitate in entomophthoromycosis.

mycotic emboli. Gastrointestinal mucormycosis is rare, with small intestinal involvement in immunocompetent adults described in only five cases in the literature, all of which were fatal, due to late diagnosis.

Entomophthorales are ubiquitous fungi causing generally chronic, subcutaneous or nasofacial infections in immunocompetent individuals in tropical and subtropical regions. The hyphae show no tendency for invading blood vessels.

Our first patient was severely debilitated with chronic obstructive pulmonary disease and chest infection and had received multiple different antibiotics prior to surgery, which probably predisposed to the fungal infection, perhaps via ingestion of fungus and invasion from the lumen into the intestinal wall. No apparent underlying intestinal disease was identifiable.

It is not possible to differentiate the various mucormycoses in tissue sections and isolation of *Mucorales* is difficult; material has to be cultured immediately.[3] Fungal cultures were not performed for our first patient. However, morphologically the appearances of the fungus were consistent with *Mucorales* and the tissue macroscopy and histology characteristic of this infection. Although Aspergillus can occasionally produce a similar tissue reaction with multinucleated giant cells, it is readily distinguished by narrow hyphae with dichotomous branching at acute angles.

Entomophthoromycosis is histologically characterized by broad, branching and sparsely septate hyphae surrounded by 'Splendore–Hoeppli' precipitates. This microscopic picture is diagnostic and distinguishes entomophthoromycosis from other fungal infections, including mucormycosis. However, culture is necessary for species identification. The eosinophilic, periodic acid–Schiff-positive material of the 'Splendore–Hoeppli' phenomenon consists mainly of immune complexes and is an expression of the host immune response.

Fifteen cases of gastrointestinal entomophthoromycosis have been reported to date, with liver involvement in only two cases.[4,5] Organisms, whenever identified, have been *Basidiobolus haptosporus*.[6] Our second patient was a farmer without any evidence of immune deficiency, systemic illness or subcutaneous lesion. We suspect that ingestion of fungi led to abscess formation in the caecum, and the hemicolectomy introduced fungi into the lymphatic and/or portal venous systems resulting in hepatic abscesses. Species identification was impossible because attempts at blood and liver aspirate cultures were unsuccessful.

Treatment of Zygomycoses requires aggressive metabolic support, antifungal therapy and surgical resection and/or debridement of necrotic involved tissue. Early diagnosis, by histological examination, is important so that life-saving antifungal therapy can be initiated.

B Azadeh
D O'B McCarthy[1]
A Dalton[2]
F Campbell

Department of Pathology, Royal Liverpool University Hospital, Liverpool, and [1]*Departments of Surgery and* [2]*Pathology, Glan Clwyd Hospital, Denbighshire, UK*

1. Ribes JA, Vanover-Sams CL, Baker DJ. Zygomycetes in human disease. *Clin. Microbiol. Rev.* 2000; 13; 236–301.

2. Lyon DT, Schubert TT, Mantia AG *et al.* Phycomycosis of the gastrointestinal tract. *Am. J. Gastroenterol.* 1979; 72; 379–394.
3. Alspaugh JA, Perfect JR. Infections due to zygomycetes and other rare fungal opportunities. *Sem. Resp. Crit. Care Med.* 1997; 18; 265–279.
4. Bittencourt AL, Ayala MAR, Ramos EAG. A new form of zygomycosis different from mucormycosis: report of two cases and review of the literature. *Am. J. Trop. Med. Hyg.* 1979; 28; 564–569.
5. de Aguiar E, Moraes WC, Londero AT. Gastrointestinal entomophthoromycosis caused by *B. haptosporus*. *Mycopathologia* 1980; 72; 101–105.
6. Lyon GM, Smilack JD, Komatsu KK *et al.* Gastrointestinal basidiobolomycosis in Arizona: clinical and epidemiological characteristics and review of the literature. *Clin. Infect. Dis.* 2001; 32; 1448–1455.

Unusually close association of ectopic intrathyroidal parathyroid gland and papillary microcarcinoma of the thyroid

Sir: We here report the unusual case of a papillary microcarcinoma of the left thyroid lobe in close proximity to an ectopic intrathyroidal parathyroid gland. A bilateral nodal goitre had been removed from a 41-year-old woman. Clinically, an adenoma was suspected within the left lobe, and the right lobe showed a nodule with decreased hormonal function ('cold' nodule) on scintigraphic evaluation. There was no history of hyperparathyroidism.

On gross examination, the largest diameters of the two roughly spindle-shaped thyroid lobes were 62 and 48 mm. Cut surfaces revealed multiple nodules measuring up to 25 mm in largest diameter. Histological analysis showed the typical picture of a '*struma colloides nodosa*' with focal regressive changes. However, the left-sided lobe contained an unusual histological finding with the close association of an encapsulated papillary microcarcinoma (follicular variant, maximum diameter 7 mm) and an ectopic (intrathyroidal) parathyroid gland (Figure 1a).

The papillary microcarcinoma showed characteristic cytological features with crowding and a ground-glass appearance of the nuclei (Figure 1b) but a completely follicular microarchitecture ('follicular variant of papillary carcinoma of the thyroid').

Immunohistochemically, the parathyroid gland revealed a typical endocrine phenotype with expression of synaptophysin (Figure 1c). The papillary carcinoma strongly expressed S100 protein, while in the adjacent normal thyroid and the parathyroid only a few scattered reticulum cells were reactive with the anti-S100 antibody (Figure 1d).

The intrathyroidal localization of parathyroid glands in general seems to be a rare finding, but there are varying reports as to its true incidence. In several studies, some of which were concerned with surgery for primary hyperparathyroidism, the frequency of intrathyroidal parathyroid glands ranged from 2.4%[1] to 8%.[2–6]

The incidence of occult papillary carcinoma in young adults (20–40 years) was 3% in an autopsy study of 138 patients.[7] In people over 40 years of age, however, this incidence increases, leading to an overall incidence of 5–24% in the whole population.[8,9]

Thus, the present case of occult papillary microcarcinoma in close proximity to an intrathyroidal parathyroid gland is a most unusual incidental finding.

H-W Bernd
H-P Horny

Institut für Pathologie,
Universitätsklinikum Schleswig-Holstein,
Lübeck, Germany

1. Lee NJ, Blakey JD, Bhuta S, Calcaterra TC. Unintentional parathyroidectomy during thyroidectomy. *Laryngoscope* 1999; 109; 1238–1240.
2. Rodriquez JM, Tezelman S, Siperstein AE *et al.* Localization procedures in patients with persistent or recurrent hyperparathyroidism. *Arch. Surg.* 1994; 129; 870–875.
3. Feliciano DV. Parathyroid pathology in an intrathyroidal position. *Am. J. Surg.* 1992; 164; 496–500.
4. Proye C, Bizard JP, Carnaille B, Quievreux JL. Hyperparathyroidism and intrathyroid parathyroid gland. 43 cases. *Ann. Chir.* 1994; 48; 501–506.
5. McIntyre RC, Eisenach JH, Pearlman NW, Ridgeway CE, Liechty RD. Intrathyroidal parathyroid glands can be a cause of failed cervical exploration for hyperparathyroidism. *Am. J. Surg.* 1997; 174; 750–753; discussion 753–754.
6. Harach HR, Vujanic GM. Intrathyroidal parathyroid. *Pediatr. Pathol.* 1993; 13; 71–74.
7. Komorowski RA, Hanson GA. Occult thyroid pathology in the young adult: an autopsy study of 138 patients without clinical thyroid disease. *Hum. Pathol.* 1988; 19; 689–696.
8. Martinez-Tello FJ, Martinez-Cabruja R, Fernandez-Martin J, Lasso-Oria C, Ballestin-Carcavilla C. Occult carcinoma of the thyroid. A systematic autopsy study from Spain of two series performed with two different methods. *Cancer* 1993; 71; 4022–4029.
9. Fink A, Tomlinson G, Freeman J-L, Rosen IB, Asa SL. Occult micropapillary carcinoma associated with benign follicular thyroid disease and unrelated thyroid neoplasms. *Mod. Pathol.* 1996; 9; 816–820.

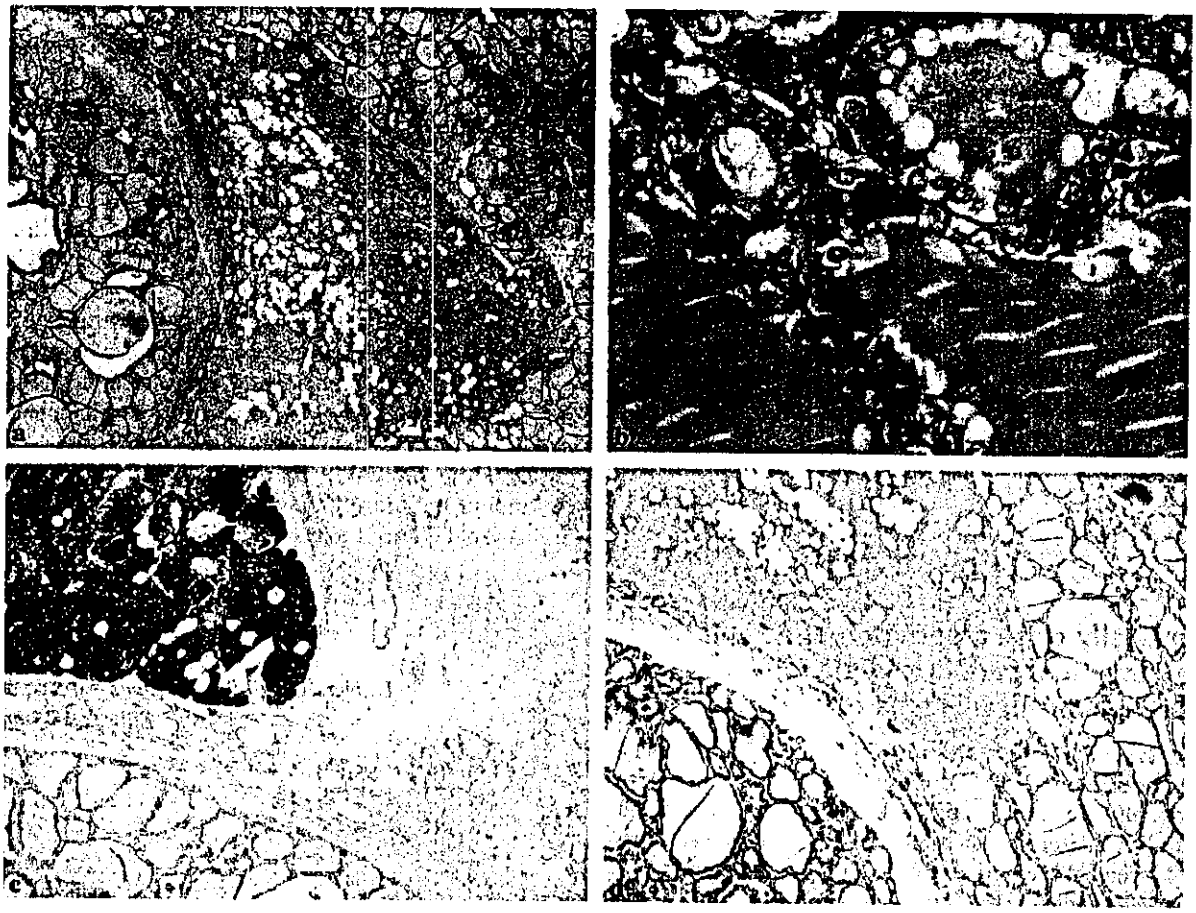

Figure 1. a, The encapsulated papillary microcarcinoma is shown on the left, the ectopic parathyroid gland in the middle, and normal thyroid tissue on the right. Note, the position of the parathyroid gland is in the immediate vicinity of the tumour capsule. b, At higher magnification, the carcinoma shows the typical nuclear features of a papillary tumour with crowding and a ground-glass appearance while the microarchitecture is completely follicular (= 'follicular variant of papillary carcinoma of the thyroid'). c, Immunostaining with an antibody to synaptophysin exhibits strong cytoplasmic staining of the cells of the parathyroid gland clearly demonstrating the endocrine nature of the cells. d, Immunostaining with an antibody to S100 protein decorates the neoplastic cells of the papillary carcinoma while the ectopic parathyroid gland and normal thyroid tissue contain only few scattered recticulum cells. The epithelial cells are not stained.

Expression of HER-2/*neu* gene and protein in salivary duct carcinomas of parotid gland as revealed by fluorescence *in-situ* hybridization and immunohistochemistry

Sir: We have read with interest the article entitled: 'Expression of HER-2/*neu* gene and protein in salivary duct carcinomas of parotid gland as revealed by fluorescence *in-situ* hybridization (FISH) and immuno histochemistry' by Skalova *et al.*[1] This work represents the first molecular assessment by FISH of *HER2* gene status in this rare and aggressive neoplasm showing a histological resemblance to ductal carcinoma of the breast. The authors studied 10 cases by immunocytochemistry and FISH. They found strong immunohistochemical positivity (3+ score) in seven cases, four of which carried *HER2* gene amplification (57%), while three were non-amplified (43%). In three cases the analysis was inconclusive.

We studied *HER2* gene status in formalin-fixed paraffin-embedded tissue sections of 18 consecutive cases of salivary duct carcinoma collected in our institution, according to previous published methodologies.[2] Eleven cases showed a score 3+, eight of which carried *HER2* gene amplification (73%), while three were non-amplified (27%). None of the immunohistochemically negative cases showed amplification.

In comparison with unselected breast carcinoma series, both the investigations outline a higher percentage of both HER-2 3+/amplified cases (25% versus

57–73%)[3] and HER2 3+/non-amplified (i.e. false-positive) cases (3% versus 27–43%)[3] in salivary duct carcinoma.

As far as the pattern of amplification is concerned, Skalova *et al.* described a homogeneously staining region (HSR) pattern in all amplified cases, while we observed three different patterns of amplification: (i) five cases presented amplified genes arranged as HSR, usually one or two per nucleus; (ii) one case showed multiple scattered single-copy HER2 signals and chromosome 17 polisomy (calculated ratio between HER2 and centromeric probe (CEP) 17 copy number was more than 2 in all tumour nuclei); (iii) two cases showed a pattern of hybridization consistent with double minutes (Figure 1), a very unusual occurrence in breast cancer.[4]

Considering the breast model where the efficiency of herceptin-based therapy is restricted to HER2 3+ or amplified cases[5] and assuming that in salivary duct carcinoma the biological basis of response to herceptin is the same as in breast cancer, we can anticipate successful use of this drug in salivary duct carcinoma. On the basis of the above-reported findings it might be expected that >50% of such patients could benefit from TKR-inhibitor therapy. However, the high rate of HER2 3+ non-amplified cases (>27%), likely to be unresponsive, necessitates FISH analysis for patient selection. Assessment by FISH is further supported by our preliminary data regarding the relationship between protein expression and the amplification pattern. Despite the presence of a 3+ immunohistochemical score, we found no HER2 protein by immunoprecipitation and Western blotting experiments in the two cases carrying double minute-related amplification. If this finding is confirmed by further experiments and since the lack of HER2 protein expression is correlated with an unsuccessful response to herceptin therapy, FISH is likely to become the assessment of choice in this salivary tumour type.

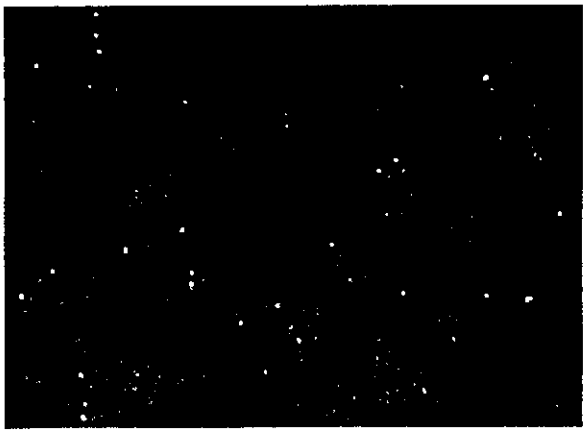

Figure 1. Example of *HER2* gene amplification in salivary duct carcinoma (HER2 signals in orange, centromeric probe (CEP) 17 signals in green). Note the pattern of amplification consistent with the presence of double minutes showing multiple clusters of amplified genes scattered over the nucleus.

ACKNOWLEDGEMENT

This work was supported by 'AIRC 2001 (Associazione Italiana per la Ricerca sul Cancro)', grant no. 420.198.122.

G P Dagrada
T Negri
E Tamborini
M A Pierotti[1,2]
S Pilotti[2]

Experimental Molecular Pathology, Department of Pathology and
[1]*Experimental Oncology Department, Istituto Nazionale per lo Studio e la Cura dei Tumori, Milano, Italy*
[2]*Senior Co-authors*

1. Skalova A, Starek I, Vanecek T *et al.* Expression of HER-2/*neu* gene and protein in salivary duct carcinomas of parotid gland as revealed by fluorescence *in-situ* hybridization and immunohistochemistry. *Histopathology* 2003; 42; 348–356.
2. Dagrada GP, Mezzelani A, Alasio L *et al.* HER-2/neu assessment in primary chemotherapy treated breast carcinoma: no evidence of gene profile changing. *Breast Cancer Res. Treat.* 2003; 80; 207–214.
3. Pauletti G, Godolphin W, Press MF *et al.* Detection and quantitation of HER-2/neu gene amplification in human breast cancer archival material using fluorescence *in situ* hybridization. *Oncogene* 1996; 13; 63–72.
4. Mitelman F. *Catalog of chromosome aberrations in cancer*, 5th ed. New York: Wiley-Liss, 1994.
5. Vogel CL, Cobleigh MA, Tripathy D *et al.* Efficacy and safety of trastuzumab as a single agent in first-line treatment of HER2-overexpressing metastatic breast cancer. *J. Clin. Oncol.* 2002; 20; 719–726.

Malignant mixed epithelial and stromal tumours of the kidney: a report of the first two cases with a fatal clinical outcome

Sir: Mixed epithelial and stromal tumour of the kidney (MESTK), a rare benign neoplasm of unknown aetiology, is a recently established entity unifying several neoplasms such as adult mesoblastic nephroma, cystic hamartoma of the pelvis, adult type cystic nephroma,

multilocular renal cysts, and solid and cystic biphasic tumour of the kidney.[1–4] In cases reported as MESTK, recurrence or fatal outcome has, to date, never been reported. Here, we present two cases of malignant MESTK with local recurrences and fatal outcomes.

The first case was in a 43-year-old Japanese woman, who had undergone radical nephrectomy for a right renal tumour and developed a local recurrent tumour 2 years later. Nine months after extirpation of the recurrent tumour she developed another local recurrence, associated with severe haemorrhage which could not be sufficiently controlled even by three trials of transarterial embolization. The recurrent tumour was found to have invaded adjacent organs allowing only palliative surgery for mass reduction. The patient died 43 months after initial nephrectomy. The second case was in a 31-year-old Japanese woman who had undergone radical nephrectomy for a tumour in the upper pole of the left kidney. Four months after the operation, she developed a local recurrent tumour, accompanied by massive ascites. She died 11 months after nephrectomy.

In case 1, the primary tumour measured approximately 70 mm in diameter, was located mainly near the renal hilus and appeared to consist chiefly of solid components. In case 2 it measured 70 × 70 × 60 mm, was generally well circumscribed and extended beyond the renal capsule. It consisted of solid and cystic components; the former was yellowish and firm and the latter was filled with haematoma.

The primary tumours of both patients were composed of proliferating spindle-shaped cells and epithelial tubular structures of various sizes (Figure 1a). The epithelial components were intermingled with the stromal components throughout the tumours. In case 1, the spindle cells had bright eosinophilic cytoplasm and fusiform nuclei with moderate atypia, formed interlacing bundles and small fascicles with high cellularity (Figure 1b) and infiltrated the renal hilar fat extensively. In case 2, the stromal components were composed of varying numbers of atypical spindle cells with clear cytoplasm that formed fascicles or whorled around the small tubules. No blastema was present. In both cases, the sizes of the epithelial tubular structures were variable, from small tubules reminiscent of normal collecting ducts to cystically dilated ducts lined by cells with a hobnail appearance (Figure 2). All the cells of the epithelial components lacked cytological atypia. It is noteworthy that tubular structures could be seen even in the extrarenally invading part of case 2's tumour and in the recurrent tumour of case 1, confirming that the tubules were not normal structures that had become involved but were integral neoplastic components of the tumours. Mitoses were conspicuous in both cases.

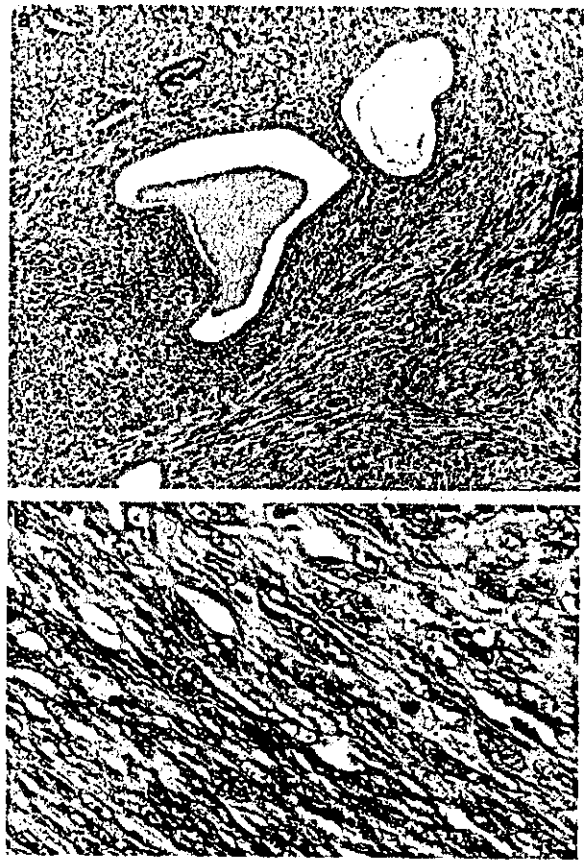

Figure 1. The primary tumour of case 1. a, The tumour is composed mainly of proliferating spindle-shaped cells and epithelial tubular or cystic structures scattered amidst the spindle cells. b, The spindle cells have eosinophilic cytoplasm and fusiform nuclei with moderate atypia and have formed small fascicles with high cellularity. Haematoxylin and eosin.

Immunohistochemically, the spindle cells of both cases were vimentin-positive, and those of case 1 were muscle-specific actin- and α-smooth muscle actin-positive. The cells of the epithelial structures of both cases were cytokeratin- and vimentin-positive and focally epithelial membrane antigen-positive.

The overall histopathological and immunohistochemical findings of these two cases were similar to those of MESTK,[2] but they consisted of more atypical spindle cells forming interlacing fascicles, bundles and whorling around the tubules with increased numbers of mitotic figures.

The differential diagnoses include leiomyosarcoma, biphasic synovial sarcoma[4] and related tumours. Although leiomyosarcoma is the most common mesenchymal tumour arising in the kidney, it contains neither neoplastic epithelial components nor entrapped tubules, because its growth is expansive rather than

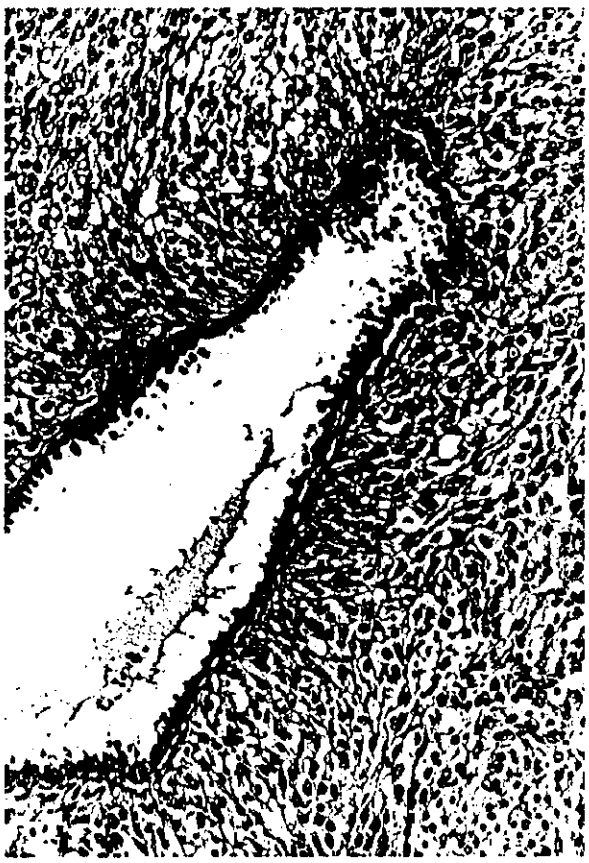

Figure 2. The primary tumour of case 2. Some cystic structures are lined by cells with a hobnail appearance. Haematoxylin and eosin.

infiltrative. Biphasic synovial sarcoma of the kidney is a rare neoplasm that contains both epithelial and stromal components.[5] Even if typical biphasic synovial sarcomas occur in the kidney, their epithelial cells are usually cuboidal or polygonal and form solid nests and glandular or tubular structures,[6] whereas the epithelial components in the present two tumours lacked obvious cytological atypia and were considered to be similar to those of the normal collecting ducts.

In conclusion, rarely, MESTK has a malignant histopathological appearance and behaves aggressively. In this situation, this tumour needs to be distinguished from leiomyosarcoma and synovial sarcoma arising in the kidney.

ACKNOWLEDGEMENTS

This study was supported by a Grant-in-Aid for the Second Term Comprehensive 10-Year Strategy for Cancer Control and a Grant-in-Aid for Cancer Research from the Ministry of Health, Labour and Welfare of Japan.

T Nakagawa
Y Kanai[2]
H Fujimoto
H Kitamura
H Furukawa[1]
S Maeda[3]
T Oyama[4]
T Takesaki[5]
T Hasegawa[2]

Urology and [1]Diagnostic Radiology Divisions, National Cancer Centre Hospital, [2]Pathology Division, National Cancer Centre Research Institute and [3]Department of Pathology, Nippon Medical School Hospital, Tokyo, and [4]Urology and [5]Pathology Divisions, Yamanashi Prefectural Central Hospital, Yamanashi, Japan

1. Michal M, Syrucek M. Benign mixed epithelial and stromal tumor of the kidney. *Pathol. Res. Pract.* 1998; 194; 445–448.
2. Adsay NV, Eble JN, Srigley JR, Jones EC, Grignon DJ. Mixed epithelial and stromal tumor of the kidney. *Am. J. Surg. Pathol.* 2000; 24; 958–970.
3. Michal M. Benign mixed epithelial and stromal tumor of the kidney. *Pathol. Res. Pract.* 2000; 196; 275–276.
4. Svec A, Hes O, Michal M, Zachoval R. Malignant mixed epithelial and stromal tumor of the kidney. *Virchows Arch.* 2001; 439; 700–702.
5. Argani P, Faria PA, Epstein JI *et al.* Primary renal synovial sarcoma: molecular and morphologic delineation of an entity previously included among embryonal sarcomas of the kidney. *Am. J. Surg. Pathol.* 2000; 24; 1087–1096.
6. Tumors of uncertain differentiation and those in which differentiation is nonmesenchymal. In Kempson RL, Fletcher CDM, Evans HL, Hendrickson MR, Sibley RK eds. *Tumors of the soft tissues (Atlas of tumor pathology, Third Series, Fascicle 30).* Washington, DC: Armed Forces Institute of Pathology, 2001; 419–501.

Neuroendocrine carcinoma of the vulva with paraganglioma-like features

Sir: Neuroendocrine tumours (NTs) of the female genital tract are relatively uncommon.[1] Particularly, NTs occurring in the vulva are extremely rare with the few cases reported in the English literature considered as Merkel cell carcinoma (MCC).[2] Here we document a neuroendocrine vulvar carcinoma with peculiar microscopic, immunohistochemical and ultrastructural features reminiscent of a paraganglioma.

A 62-year-old woman presented with a 20-mm soft, painful lump located in the right upper portion of the labia majora. Abdominothoracic computed tomography (CT) scan excluded the possibility of it being a metastasis from a primary tumour elsewhere. An excisional biopsy was performed and a diagnosis of neuroendocrine carcinoma made. Three months later the neoplasm recurred locally and right inguinal lymphadenopathy was noted. Treatment consisted of radical vulvectomy followed by local radiotherapy. Eight months later a total body CT scan revealed an enlargement of the abdominal and mediastinal lymph nodes. Nineteen months after the original diagnosis the patient is still alive with multiple abdominal and thoracic metastases.

Histologically, the tumour involved the dermis and subcutis and showed a prevalent organoid or 'Zellballen' pattern of growth (Figure 1a). Occasionally, hypercromatic, slender cells, resembling sustentacular cells, outlined the neoplastic nests.

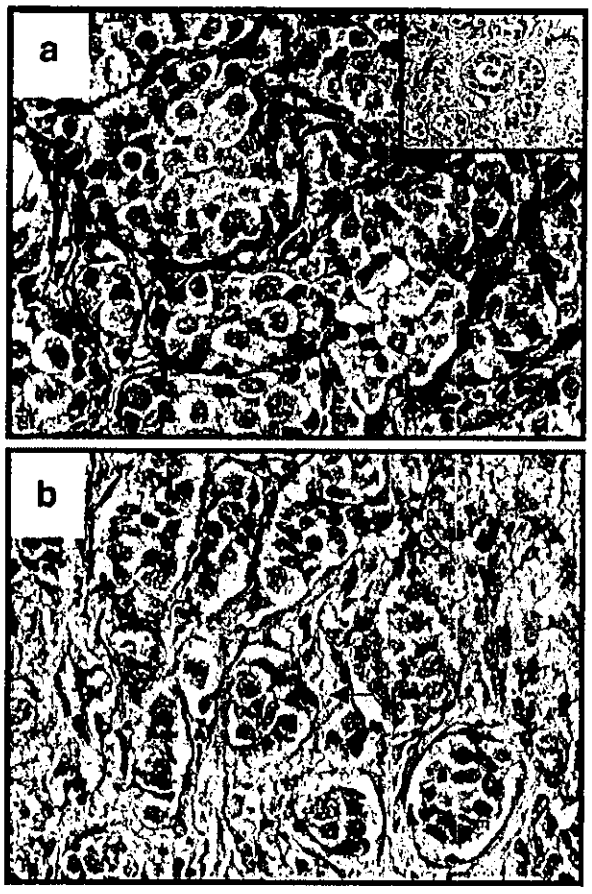

Figure 1. a Neoplastic cells were mainly disposed in organoid nests. Inset: rare glandular structures were found in another microscopic field. b, Immunohistochemically, S100 protein outlined a residual stellate/dendritic cell at the periphery of a tumour nest (arrow).

Tumour cells were medium in size, with abundant clear to eosinophilic cytoplasm; nuclei were round to oval with fine chromatin and occasional nucleoli. Mitotic figures, apoptotic bodies, foci of tumour necrosis, vascular invasion, and occasional glandular or pseudoglandular structures (Figure 1a, inset) were observed. Metastatic nodal disease was morphologically similar to the primary vulvar neoplasm.

Neoplastic cells were immunoreactive for cytokeratin 8 and 18, carcinoembryonic antigen (CEA), synaptophysin, PGP9.5 and neuron-specific enolase but were negative for cytokeratin 20, chromogranin A, and TTF-1. Protein S100 decorated occasional cells at the periphery of the 'Zellballen' (Figure 1b).

Electron microscopy was performed from a paraffin block. Tumour cells contained numerous dispersed cytoplasmic membrane-bound dense granules and exhibited features of epithelial differentiation including cell junctions. Moreover, electron microscopy showed the presence of long, slender sustentacular cells, outlining the epithelial nests.

On the basis of the morphological, immunohistochemical, ultrastructural and clinical findings a final diagnosis of neuroendocrine carcinoma of the vulva with paraganglioma-like features was made. The differential diagnosis included metastatic neuroendocrine carcinoma, malignant paraganglioma and MCC. Careful clinical evaluation and the absence of a previous history of a neuroendocrine neoplasm help to rule out a metastasis.

The 'Zellballen' growth pattern and the presence of sustentacular cells suggested a diagnosis of paraganglioma. A case of paraganglioma without malignant features occurring in the vulva has been reported.[3] However, in the present case the presence of glands, the strong cytokeratin and CEA immunoreactivity, and the ultrastructurally evident desmosomal junctions strongly supported an epithelial origin of the lesion. Paraganglioma stains for neuroendocrine markers, but is not usually reactive for cytokeratin and CEA. Although occasional examples of paraganglioma have been reported to be immumoreactive for keratin,[4] CEA immunostaining has never been described in this tumour.[5] Moreover, it is noteworthy that the presence of sustentacular cells is not exclusive to paragangliomas.[6]

Although the few reports describing primary neuroendocrine carcinoma of the vulva support its origin from epidermal Merkel cells, this case did not show the typical immunohistochemical and ultrastructural features of MCC.[2]

The origin of primary vulvar neuroendocrine carcinomas is particularly intriguing.[7,8] In the present case the apparent lack of any relationship with vestibular glands and the absence of morphological features other than neuroendocrine strongly support an origin from solitary or aggregated cells of the diffuse/dispersed neuroendocrine system.

Whether the present case is simply a histological curiosity or has clinical significance is a moot point. We suggest that the diagnosis of neuroendocrine carcinoma, even with an unusual morphological appearance, should always be taken into account, since these tumours have a highly malignant clinical course, with disseminated disease usually occurring within 1 year following diagnosis.

P G Nuciforo
F Fraggetta[1]
R Fasani
P Braidotti
G Nuciforo[2]

Department of Medicine, Surgery and Dental Sciences, University of Milan, A. O. S. Paolo and IRCCS Ospedale Maggiore, Milan, [1]*Department of Pathology, Ospedale Cannizzaro, Catania, and* [2]*Department of Pathology, A.O. Vittorio Emanuele-S. Bambino, Catania, Italy*

1. Eichhorn JH, Young RH. Neuroendocrine tumors of the genital tract. *Am. J. Clin. Pathol.* 2001; 115; S94–S112.
2. Hierro I, Blanes A, Matilla A, Munoz S, Vicioso L, Nogales FF. Merkel cell (neuroendocrine) carcinoma of the vulva. A case report with immunohistochemical and ultrastructural findings and review of the literature. *Pathol. Res. Pract.* 2000; 196; 503–509.
3. Colgan TJ, Dardick I, O'Connell G. Paraganglioma of the vulva. *Int. J. Gynecol. Pathol.* 1991; 10; 203–208.
4. Chetty R, Pillay P, Jaichand V. Cytokeratin expression in adrenal phaeochromocytomas and extra-adrenal paragangliomas. *J. Clin. Pathol.* 1998; 51; 477–478.
5. LaGuette J, Matias-Guiu X, Rosai J. Thyroid paraganglioma: a clinicopathologic and immunohistochemical study of three cases. *Am. J. Surg. Pathol.* 1997; 21; 748–753.
6. Al-Khafaji B, Noffsinger AE, Miller MA *et al.* Immunohistologic analysis of gastrointestinal and pulmonary carcinoid tumors. *Hum. Pathol.* 1998; 29; 992–999.
7. Pearse AGE, Takor TT. Embriology of the diffuse neuroendocrine system and its relationship to the common peptides. *Fed. Proc.* 1979; 32; 2288–2294.
8. Slone S, Reynolds L, Gall S *et al.* Localization of chromogranin, synaptophysin, serotonin, and CXCR2 in neuroendocrine cells of the minor vestibular glands: an immunohistochemical study. *Int. J. Gynecol. Pathol.* 1999; 18; 360–365.

Myxoid Epithelioid Gastrointestinal Stromal Tumor (GIST) With Mast Cell Infiltrations: A Subtype of GIST With Mutations of Platelet-Derived Growth Factor Receptor Alpha Gene

SHINJI SAKURAI, MD, TADASHI HASEGAWA, YUJI SAKUMA, YUTAKA TAKAZAWA, ATSUSHI MOTEGI, TAKASHI NAKAJIMA, KEN SAITO, MASASHI FUKAYAMA, AND TADAKAZU SHIMODA

We analyzed 30 gastrointestinal stromal tumors (GISTs) that were immunohistochemically weak or negative for KIT. Histologically, all 30 GISTs consisted of epithelioid tumor cells in at least a part of the tumor. The tumor cells showed different morphologies and arranged themselves in different histological patterns. In 20 of the 30 GISTs, round or oval epithelioid tumor cells often showed a less cohesive pattern of growth and showed eosinophilic cytoplasm and peripherally placed nuclei with myxoid stroma, whereas in the remaining 10 cases, tumor cells were arranged in a more cohesive pattern without myxoid stroma. The former type of tumors is called *myxoid epithelioid GISTs* in this study. Subsequent mutational analyses showed that the platelet-derived growth factor receptor alpha (*PDGFRA*) gene mutations in exon 12 or exon 18 were identified in 20 (66.7%) of the 30 GISTs, and especially in 18 (90%) of the 20 myxoid epithelioid GISTs. Moreover, 17 (85%) of the 20 myxoid epithelioid GISTs were accompanied by mast cell infiltrations within the tumor nodules. In the remaining cases, 2 (6.7%) of the 30 GISTs had c-*kit* gene mutations in exon 11, and no mutation was found in 8 (26.7%) of 30 GISTs. None of the patients with myxoid epithelioid GISTs died of disease. These results suggest that myxoid epithelioid GISTs are a distinct subtype of GISTs that are closely correlated with the *PDGFRA* gene mutation and that recognition of such histological characteristics should be helpful for molecular subclassification of GISTs that are important for molecular targeting therapy by imatinib mesylate (STI571). HUM PATHOL 35:1223-1230. © 2004 Elsevier Inc. All rights reserved.

Key words: **GISTs, myxoid epithelioid, mast cell infiltration, *PDGFRA* gene mutation.**

Abbreviations: **GISTs, gastrointestinal stromal tumors; PDGFRA, platelet-derived growth factor receptor alpha; ICCs, interstitial cells of Cajal; PCR, polymerase chain reaction.**

Gastrointestinal stromal tumors (GISTs) are the most frequent nonepithelial neoplasm in the stomach and intestine.[1-5] In the past, most GISTs were thought to originate from smooth muscle, based on their histological features. However, recent reports clarified the close relationship between GISTs and interstitial cells of Cajal (ICCs), which play important roles, such as as the pacemaker that enables cooperative peristalsis or as the mediator of nitric oxide–mediated transmission from nerve terminals to smooth muscle cells in the gastrointestinal tract.[6,7] Simultaneous expression of specific molecules such as KIT, CD34, the embryonic isoform of myosin heavy chain (SMemb), and nestin in both ICCs and GISTs[8-12] leads us to consider that GISTs may develop from ICCs or their progenitor cells. In previous reports, about 90% of GISTs were immunohistochemically positive for KIT,[8-12] and mutations of the c-*kit* gene have been found in most of these KIT-positive GISTs.[13] Recently, mutations of the platelet-derived growth factor receptor alpha (*PDGFRA*) gene encoding platelet-derived growth factorα have been reported in GISTs that are negative for c-*kit* gene mutations.[14,15]

Histopathologically, most GISTs consist of spindle tumor cells with acidophilic fibrillary cytoplasm and elongated or cigar-shaped nuclei with perinuclear vacuoles. In our experience, these typical GISTs are usually KIT positive by immunohistochemical staining. On the other hand, tumor cells show pleomorphic or epithelioid histology in rare cases of GISTs, and such histology is sometimes difficult for pathologists to diagnose. In such cases, an immunohistochemically positive result for KIT is a useful marker for the diagnosis of GISTs.

However, in our previous analyses, we found that KIT immunoreactivity in epithelioid cells of GISTs was weaker than in spindle cells in the same tissue sections or other tumors. Moreover, some GISTs were completely negative for KIT. Lack of the c-*kit* gene mutation had also been reported in GISTs with an epithelioid component.[16] In such cases, accuracy of the diagnosis of GISTs may be questionable. In this study, to clarify the clinicopathologic features and molecular genetic background of such tumors, we analyzed 27 cases of

From the Department of Pathology, Jichi Medical School, Tochigi, Department of Pathology, National Cancer Center Research Institute and Hospital, Tokyo, Department of Pathology, Graduate School of Medicine, University of Tokyo, Tokyo, and Department of Tumor Pathology, Gunma University Graduate School of Medicine, Maebashi, Gunma, Japan. Accepted for publication July 1, 2004.

Supported by a Grant-in-Aid for Scientific Research from the Ministry of Education, Science, Sports, and Culture of Japan and by a Grant-in-Aid for Cancer Research from the Ministry of Health, Labor and Welfare of Japan.

Address correspondence and reprint requests to Shinji Sakurai, MD, 3311-1 Yakushiji, Minamikawachi-machi, Kawachi-gun, Tochigi 329-0498, Japan.

0046-8177/$—see front matter

doi:10.1016/j.humpath.2004.07.008

TABLE 1. Risk Category for Gastrointestinal Stromal Tumor Based on the MIB-1 Grading System and Tumor Size

	Tumor size (cm)		
Grade*	≤5	<5-≤10	>10
Low	Low risk	Intermediate risk	High risk
High	High risk	High risk	High risk

*Low grade, MIB-1–labeling index of <10% and no tumor necrosis; high grade MIB-1–labeling index of ≥10% or tumor necrosis.

GISTs showing weak or negative staining for KIT. From the results of histological findings and mutational analyses of the c-*kit* and the *PDGFRA* gene, we showed that specific histology of GISTs was closely correlated with the *PDGFRA* gene mutation and termed such GISTs *myxoid epithelioid GISTs.*

MATERIALS AND METHODS

KIT-Weak or KIT-Negative GISTs

The study was approved by the research ethics committee of Jichi Medical School. Of the 303 GISTs collected at Jichi Medical School Hospital, National Cancer Center Hospital, and related hospitals, all of which were analyzed by the immunohistochemical techniques described in this section, 30 (9.9%) primary GISTs showing negative or weak immunostaining for KIT were selected. A consensus judgment was adopted as the proper immunohistochemical score of the tumor on the basis of strength: 0, negative; 1+, weak staining; 2+, moderate staining; 3+, strong staining. Tissue mast cells, which stain 2+ or 3+, were used as internal positive controls for KIT. The distribution of positive cells was also recorded in an effort to impart the diffuse or focal nature of the positive cells: sporadic (positive cells <10%), focal (10% to <50% positive cells), or diffuse (50% positive cells). The immunohistochemical scores of 0 and 1+ with focal to diffuse distribution were considered to be KIT-weak or KIT-negative GISTs.

Of these, 29 GISTs were surgically resected from 29 patients, and the remaining 1 was from an autopsy case in which the patient died of hypoxic encephalopathy (case 22). The sites of the primary tumors were the stomach (n = 26), esophagus (n = 1), small intestine (n = 1), and omentum (n = 2). One patient (case 17) was treated with imatinib mesylate because of the residual tumor in the omentum. Formalin-fixed and paraffin-embedded specimens were used for histopathologic and immunohistochemical studies and for mutational analyses for the c-*kit* and *PDGFRA* genes. All GISTs were graded as high, intermediate, or low risk according to tumor size and to the MIB-1 grading system described elsewhere,[17] based on tumor differentiation, existence of tumor necrosis, and proliferating activity as estimated by Ki-67 (MIB-1) immunohistochemistry. Briefly, high-risk GISTs are >10 cm or are high grade (MIB-1–labeling index = 10% or tumor necrosis), intermediate-risk GISTs are >5 cm to 10 cm and are low grade (MIB-1–labeling index of <10% and no tumor necrosis), and low-risk GISTs are 5 cm and are low grade (Table 1).

Immunohistochemical Study

Immunohistochemical evaluation was performed by the avidin-biotin-peroxidase complex method in 3-μm-thick sections of formalin-fixed and paraffin-embedded specimens of GISTs and other mesenchymal tumors. We used polyclonal antibodies for KIT (DakoCytomation, Glostrup, Denmark: working dilution, 1:50; IBL, Fujioka, Japan: working dilution, 1:100), and a monoclonal antibody for CD34 (Becton Dickinson, Mountain View, CA: working dilution, 1:20). Cellular differentiation in GISTs was characterized by using the following antibodies: α-smooth muscle actin (DakoCytomation; monoclonal; working dilution, 1:500) and desmin (DakoCytomation; monoclonal; working dilution, 1:100) as markers for smooth muscle cells and by using the S100 protein (DakoCytomation; polyclonal, 1:1000) as a marker for Schwann cells. Ki-67 (MIB-1; MBL, Nagaoya, Japan: monoclonal, 1:100) was used to assess the proportion of proliferating cells, and the MIB-1–labeling index was estimated as reported elsewhere.[17] For antigen retrieval, formalin-fixed sections were pretreated in a microwave oven before incubation with the primary antibody.

We also performed toluidine blue staining for detection of mast cell infiltrations in GISTs. In the same KIT-stained sections of GISTs, we found many mast cell infiltrations between tumor cells. To accurately evaluate mast cell infiltrations in the tumors, toluidine blue staining was performed on all 3-μm-thick sections of formalin-fixed and paraffin-embedded specimens of GISTs in this study. For comparison, 24 cases of KIT-positive typical GISTs, all of which had c-*kit* gene mutations (23 in exon 11 mutations and 1 in exon 9) as shown by reverse-transcription polymerase chain reaction (PCR) and direct sequencing (data not shown), were also analyzed.

Sequencing Analyses of the C-*Kit* and *PDGFRA* Genes

Previously identified mutational hot spots in the c-*kit* and the *PDGFRA* gene in GISTs were analyzed. Genomic DNA was extracted from the 30 formalin-fixed and paraffin-embedded tumor tissues, by a standard proteinase K digestion method. Then the genomic DNA was amplified by PCR with the primers listed in Table 2 to amplify exons 9, 11, 13, and 17 of the c-*kit* gene and exons 12 and 18 of the *PDGFRA* gene. Each of the amplified fragments was purified from a polyacrylamide gel, and direct sequencing was performed with a Thermo Sequenase II Dye Terminator Cycle Sequencing Premix Kit (Amersham Biosciences, Piscataway, NJ) and with an ABI

TABLE 2. Sequences of Primers Used in This Study

Exon	Sequence
	c-kit
Exon 9F	5'-ATGCTCTGCTTCTGTACTGCC-3'
Exon 9R	5'-CAGAGCCTAAACATCCCCTTA-3'
Exon 11F	5'-CCAGAGTGGTCTAATGACTG-3'
Exon 11R	5'-ACCCAAAAAAGGTGACATGGA-3'
Exon 13F	5'-GATCAGTTTGCCAGTTGTGC-3'
Exon 13R	5'-AGACGGGCTTTACCTCCAAATG-3'
Exon 17F	5'-TGTATTCAGAGAGACTTGGG-3'
Exon 17R	5'-GGATTTACATTATGAAAGTCACAGG-3'
	PDGFRA
Exon 12F	5'-TCCAGTCACTGTGCTGCTTG-3'
Exon 12R	5'-GCAAGGGAAAAGGGAGTCTT-3'
Exon 18F	5'-ACCATGGATCAGCCAGTCTT-3'
Exon 18R	5'-AAGTGTGGGAGGATGAGCCTG-3'

Abbreviation: PDGFRA, platelet-derived growth factor-α.

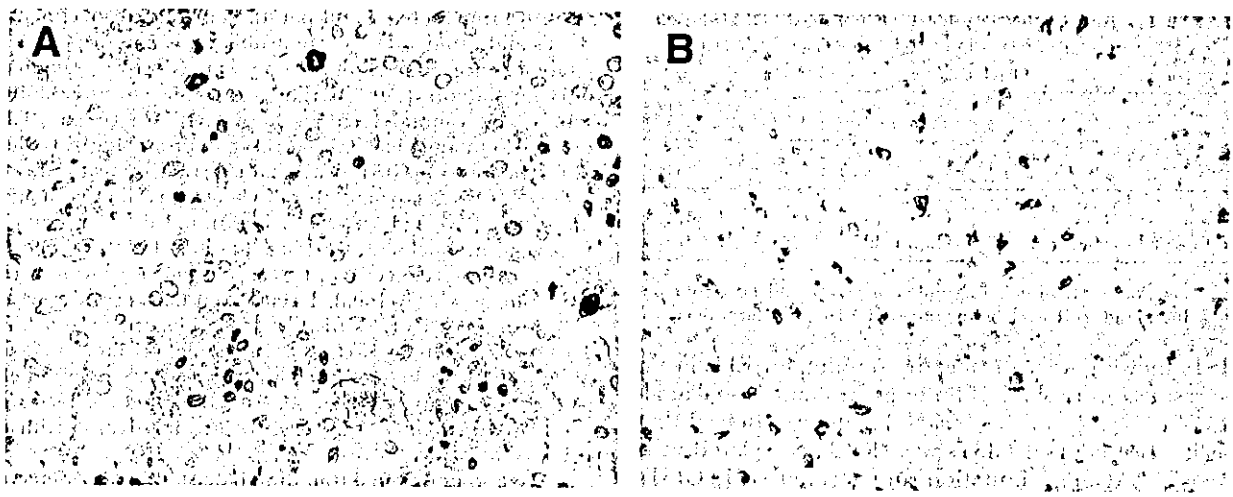

FIGURE 1. Immunostaining for KIT. All 27 gastrointestinal stromal tumors in this study were weak (A) or negative (B) for KIT. Strong immunoreactivity to KIT was observed in infiltrating mast cells in both cases.

PRISM 377 DNA Sequencer (Applied Biosystems, Foster City, CA), using the same primers as were used for PCR. All sequencing reactions were performed in both the forward and reverse directions.

Statistical Analyses

For the statistical analyses, we compared GISTs with and without myxoid epithelioid patterns (described in the results) and compared GISTs with or without the *PDGFRA* gene mutations. Gender, primary site, tumor grade, histological types, immunohistochemical phenotypes, and the existence of mast cell infiltrations were evaluated by Fisher's exact test or by χ^2 test. Age at surgery, maximum size of the tumors, and the MIB-1–labeling indexes were compared by Mann-Whitney U test.

RESULTS

Of the 30 GISTs examined in this study, 26 showed weak positive immunostaining for KIT according to our criteri, and the remaining cases (cases 20, 22, 25, and 26) were completely negative for KIT (Fig 1A and B). The clinicopathologic data resulting from the immunohistochemistry and mutational analyses of the *c-kit* and *PDGFRA* genes are presented in Table 3. The MIB-1–labeling index ranged from 1% to 21%. According to the criteria described above, 10 of the 30 tumors were classified as low risk, 6 as intermediate risk, and the remaining as high risk.

Histologically, all 30 GISTs showed epithelioid tumor cells in at least part of the tumor. Of these, we noticed that the tumor cells showed different morphology and arranged themselves in different patterns in each case with or without myxoid stroma. In cases 1, 2, 7, 11, 14, 19, 29, and 30, tumors consisted of both spindle and epithelioid tumor cells in varying ratios, and in the remaining cases, epithelioid cells occupied most parts of the tumor. In cases 1, 2, 3, 5, 7, 11, 17, 19, 27, and 29, the epithelial components of the tumor cells were mostly cohesive and arranged themselves in a sheetlike structure. Tumor cells in these cases showed clear or eosinophilic cytoplasm and centrally or peripherally placed nuclei (Fig. 2A).

On the other hand, in the remaining 17 cases of GISTs in this study, round or oval epithelioid tumor cells often showed a less cohesive pattern of growth and showed eosinophilic cytoplasm and peripherally placed nuclei with myxoid stroma. Multinucleated tumor cells were also seen in these tumors (Fig 2B), for which we used the term *myxoid epithelioid GISTs* in this study. Cases 6, 11, and 15, in which the myxoid epithelioid pattern was seen only in a part of the tumor, were also placed in this category.

Immunohistochemical Phenotypes

Of the 30 GISTs in the present study, 25 tumors were positive for CD34, and 13 tumors were weakly or focally positive for α-smooth muscle actin. Only 1 case was weakly positive for S100 protein, and 2 cases were weakly positive for desmin.

Mutations of the C-*kit* and *PDGFRA* Genes

Of the 30 GISTs examined here, 2 GISTs had *c-kit* gene mutations in exon 11 that were point mutations or in-frame deletions. *PDGFRA* gene mutations were found in 20 GISTs: 2 tumors had the same missense point mutation at codon 561 in exon 12, and the remaining tumors had in-frame deletions from codon 842 to 845 or had missense point mutations at codon 842 in exon 18. These are the same mutations of the *PDGFRA* gene in GISTs without the *c-kit* gene mutation, as previously reported. In the remaining 8 GISTs, mutations were not found in any exons of *c-kit* or *PDGFRA*.

TABLE 3. Clinicopathological Data Resulting From Immunohistochemistry and Mutational Analysis of the C-Kit and PDGFRA Gene In 27 Cases of KIT-Weak or KIT-negative GISTs

Case No.	Gender	Age	Primary Site	MIB-1 Size	MIB-1 LI (%)	MIB-1 Risk	Histology	Immunohistochemistry KIT	CD34	S100	SMA	Desmin	Mutations Gene	Mutations Site	Mast Cell Infiltration	Follow-Up Results (mo)
1	M	46	Small intestine	2.5	21	High	Spindle-cohesive epithelioid	Weak	+	+	−	−	—		—	DOD (22)
2	M	57	Esophagus	1.1	18	High	Spindle-cohesive epithelioid	Weak	+	−	−	−	c-kit	Exon 11 K558S, del V559	—	AW (16)
3	M	68	Stomach	7.5	<1	Int	Cohesive epithelioid	Weak	−	−	−	−	—		—	DOD (62)
4	M	60	Stomach	3.5	<1	Low	Myxoid epithelioid	Weak	+	−	−	−	PDGFRA	Exon 18 del DIMH842-845	+*	DOUD (564)
5	M	73	Stomach	8	8	Low	Cohesive epithelioid	Weak	−	−	+	−	—		—	AW (356)
6	M	46	Stomach	3	5	Low	Cohesive-myxoid epithelioid	Weak	+	−	−	−	—		—	AW (202)
7	F	71	Stomach	3.5	3	Low	Spindle-cohesive epithelioid	Weak	+	−	−	−	—		—	AW (190)
8	F	76	Stomach	2	9	Low	Myxoid epithelioid	Weak	+	−	+	−	PDGFRA	Exon 18 D842V	+−†	AW (143)
9	M	43	Stomach	2.5	5	Low	Myxoid epithelioid	Weak	+	−	−	−	PDGFRA	Exon 18 D842V	−	AW (118)
10	M	44	Stomach	10	5	Int	Myxoid epithelioid	Weak	+	−	−	−	PDGFRA	Exon 18 del DIMH842-845	+ +	AW (101)
11	M	60	Stomach	12.5	3	High	Spindle-myxoid epithelioid	Weak	+	−	+	−	PDGFRA	Exon 18 del DIMH842-845, D846E	+	AW (96)
12	M	65	Stomach	3	3	Low	Myxoid epithelioid	Weak	+				—		+	AW (75)
13	M	50	Stomach	21	10	High	Myxoid epithelioid	Weak	+		+	+	PDGFRA	Exon 18 del DIMH842-845	+	AW (43)
14	M	62	Stomach	2.5	15	High	Spindle-cohesive epithelioid	Weak	+			+	c-kit	Exon 11 del MYEV552-555	—	AW (6)
15	M	46	Stomach	1.2	11	High	Cohesive-myxoid epithelioid	Weak	+		+	−	PDGFRA	Exon 18 D842V	—	AW (6)
16	F	73	Omentum	4	3	Low	Myxoid epithelioid	Weak	+	−	+	−	PDGFRA	Exon 18 D842V	+ −	AW (4)
17	M	52	Omentum	>20	4	High	Cohesive epithelioid	Weak	−	−	−	−	PDGFRA	Exon 18 del DIMH842-845	+	AW (13)
18	F	80	Stomach	3.7	3	Low	Myxoid epithelioid	Weak	+	−	−	−	PDGFRA	Exon 12 V561D	+	AW (3)
19	M	51	Stomach	2.5	2	Low	Spindle-cohesive epithelioid	Weak	+	−	−	−	—		—	DOUD (171)
20	M	65	Stomach	8	1	Int	Myxoid epithelioid	—	−	−	−	−	PDGFRA	Exon 12 V561D	+ −	ND
21	M	49	Stomach	8	14	High	Myxoid epithelioid	Weak	+	−	−	−	PDGFRA	Exon 18 del DIMH842-845	+	AW (12)
22	M	66	Stomach	1.2	19	Low	Myxoid epithelioid	—				−	PDGFRA	Exon 18 D842V	+	ND
23	M	54	Stomach	1.1	3	Low	Myxoid epithelioid	Weak	+			−	PDGFRA	Exon 18 D842V	+ +	AW (12)
24	M	74	Stomach	6	4.5	Int	Myxoid epithelioid	Weak	+			−	PDGFRA	Exon 18 D842V	+	AW (24)
25	F	36	Stomach	2.2	7.5	Low	Myxoid epithelioid	—	+	−	−	−	PDGFRA	Exon 18 del DIMH842-845	+	AW (9)
26	M	57	Stomach	6	5	Int	Myxoid epithelioid	—	+			−	PDGFRA	Exon 18 del DIMH842-845	+	AW (8)
27	F	64	Stomach	4	<1	Low	Cohesive epithelioid	Weak	+				—	—	AW (30)	
28	M	69	Stomach	6.5	2	Int	Myxoid epithelioid	Weak	+	−	+	−	PDGFRA	Exon 18 D842V	+	AW (1)
29	M	50	Stomach	4	5	Low	Spindle-cohesive epithelioid	Weak	+		+		PDGFRA	Exon 18 D842V	—	AW (3)
30	M	75	Stomach	2.3	9	Low	Spindle-myxoid epithelioid	Weak	+		+	−	PDGFRA	Exon 18 D842V	+	AW (1)

Abbreviations: PDGFRA, platelet-derived growth factor-α; GIST, gastrointestinal stromal tumor; LI, labeling index; SMA, smooth muscle actin; DOD, died of disease; del, deletion; AW, alive and well; Int, intermediate; DOUD, died of unrelated disease; ND, no data available.

*For most cell infiltration instances.

†Numerous mast cell infiltration instances present within a tumor nodule.

GISTs With or Without Mast Cell Infiltration

Mast cells were clearly detected by their characteristic metachromatic staining with toluidine blue. Infiltration of mast cells within the tumor nodules was observed in 18 of the 30 GISTs (60%; Fig 3A), although the number of infiltrating mast cells was varied in each case (Table 3). In contrast, no mast cell infiltration of 21 KIT-positive GISTs with *c-kit* gene mutations was observed (Fig 3B).

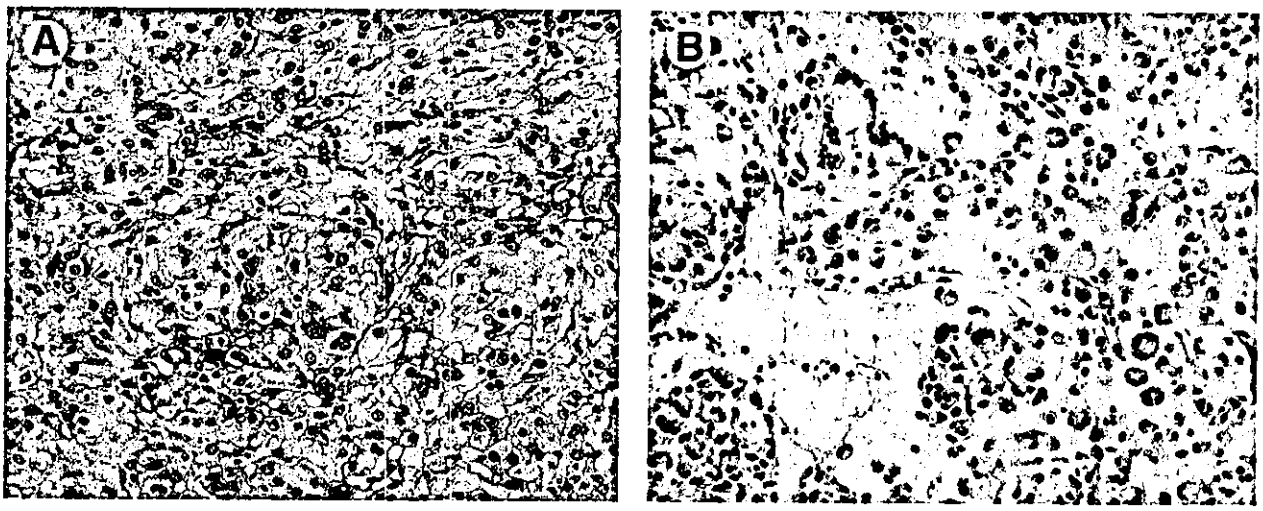

FIGURE 2. Epithelioid components of gastrointestinal stromal tumors in this study showed different histology. (A) Tumor cells in this case showed clear cytoplasm and centrally or peripherally placed nuclei and were mostly cohesive and arranged themselves in a sheetlike structure. (B) Tumor cells in other cases showed less cohesive patterns of growth and showed eosinophilic cytoplasm and peripherally placed nuclei with myxoid stroma. Multinucleated tumor cells were also seen in these tumors. Hematoxylin and eosin staining.

KIT-Weak or KIT-Negative GISTs With or Without Myxoid Epithelioid Patterns

The clinicopathologic data including other immunohistochemical data, the existence of mast cell infiltrations in the tumor nodules, and mutations of the *c-kit* or *PDGFRA* gene were compared between the 27 GISTs with or without myxoid epithelioid patterns (Table 4). The gender, age at initial operation, primary sites and sizes of tumors, MIB-1–labeling index and tumor risk, and immunohistochemical phenotypes were not different between the 2 groups. Mast cell infiltrations within the tumor nodules were preferentially observed in the GISTs with a myxoid epithelioid pattern ($P < 0.0001$). Only 1 weakly KIT-positive large GIST (case 19) without a myxoid epithelioid pattern was accompanied by mast cell infiltration. The presence or site of mutations in the *c-kit* or *PDGFRA* genes was significantly different between GISTs with and without a myxoid epithelioid pattern ($P < 0.0001$). Mutations in the *PDGFRA* gene were preferentially found in the GISTs with a myxoid epithelioid pattern (18 of 20, 90%), whereas only 2 of the 10 GISTs without a myxoid epithelioid pattern had a *PDGFRA* gene mutation (case 17). Two cases in GISTs without a myxoid epithelioid pattern (cases 2, 14) had a point mutation or an in-frame deletion in exon 11 of the *c-kit* gene.

Prognosis of the patients with KIT-weak or KIT-negative GISTs was as follows. Twenty-eight patients were followed for 1 to 364 months (mean, 82 months; median, 42 months). Four of the 28 patients died dur-

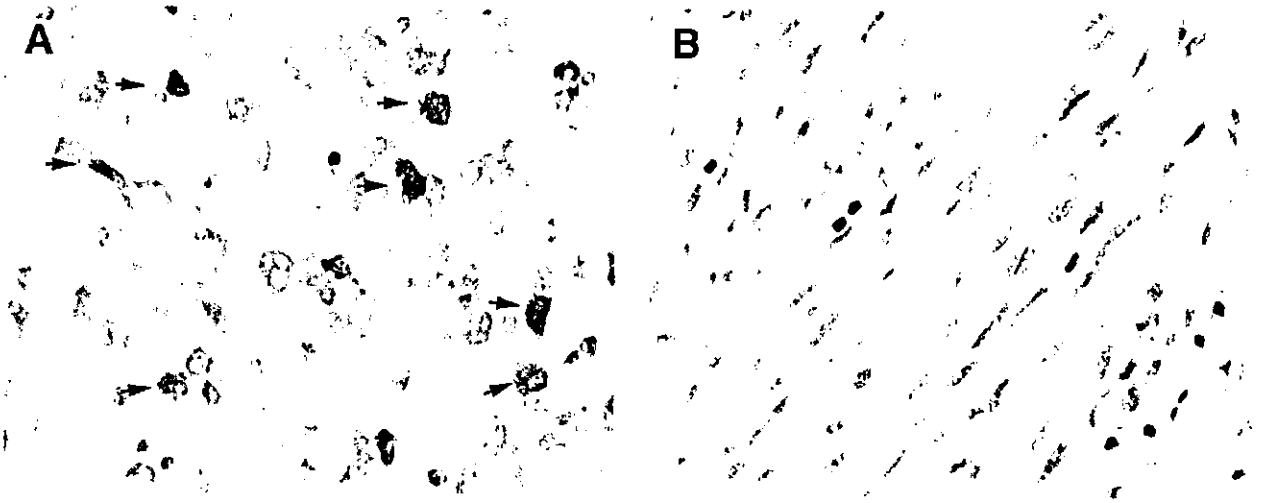

FIGURE 3. Mast cell infiltrations were frequently observed in KIT-weak or KIT-negative gastrointestinal stromal tumors (GISTs; arrow; A) but not in KIT-positive GISTs with *c-kit* gene mutations (B). Toluidine blue staining.

TABLE 4. Comparison of Clinicopathological and Immunohistochemical Data and Mutational Analysis of the C-Kit and PDGFRA Gene Between Myxoid Epithelioid GISTs and Others

Variable	KIT-Weak or KIT-Negative GISTs		*P* Value
	Myxoid Epithelioid GISTs (n = 20)	Others (n = 10)	
Gender (male:female)	16:4	9:1	NS
Age (yr)	36-80 (average 59.5)	46-73 (average, 59.4)	NS
Site (eso/st/SI/ome)	0/20/0/1	1/7/1/1	NS
Size	5.4 ± 4.8	5.4 ± 5.3	NS
MIB-1 LI	5.4 ± 3.5	7.8 ± 7.5	NS
Grade (high/int/low)	4/5/11	4/1/5	NS
Immunohistory			
CD34	18/20	7/10	NS
SMA	10/20	3/10	NS
S100	0/20	1/10	NS
Desmin	1/20	1/10	NS
Mast cell infiltration	17/20	1/10	0.0001
Mutation (c-kit/PDGFRA/negative)	0/18/2	2/2/6	0.0001

Abbreviations: PDGFRA, platelet-derived growth factor-α; GIST, gastrointestinal stromal tumor; NS, statically not significant; eso, esophagus; St, stomach; SI, small intestine; LI, labeling index; SMA, smooth muscle actin.

ing the follow-up period, of which 2 deaths were caused by the primary disease (cases 1 and 3, each 22 and 62 months after initial operations) and the remaining deaths were caused by unrelated disease (cases 4 and 19). GISTs in cases 1 and 3 had no myxoid epithelioid component in the tumor cells or mutations in the *c-kit* and *PDGFRA* genes. None of the patients with myxoid epithelioid GISTs or GISTs with *PDGFRA* gene mutations died of disease during follow-up periods, although 1 patient had a residual tumor at the primary site (case 17).

DISCUSSION

In recent years, the diagnosis and treatment of GISTs has advanced and changed dramatically. Most GISTs consist of spindle cells showing fascicular patterns and are immunohistochemically positive for KIT.[8-12] Moreover, gain-of-function mutations in the *c-kit* gene are found in these KIT-positive GISTs.[8,13] Now, GISTs are defined as KIT-positive mesenchymal tumors in the gastrointestinal tract and are distinguished from other mesenchymal tumors. Recently, molecular targeting treatments with imatinib mesylate (STI571), which is a KIT tyrosine kinase inhibitor, have been given to patients with KIT-positive GISTs, with reports of significant effectiveness for metastatic and unresectable GISTs.[18,19]

However, it is known that some GISTs are immunohistochemically weak or negative for KIT. In such cases, the accurate diagnosis of GISTs might be difficult for pathologists, although the pathologic diagnosis is indispensable for correctly prescribing imatinib mesylate.

More recently, *PDGFRA* gene mutations have been reported in some GISTs without *c-kit* gene mutations that also can be effectively treated with imatinib mesylate.[14,15,20] However, the clinicopathologic and histological characteristics of GISTs with *PDGFRA* gene mutations have not been fully analyzed previously.

Overall, 30 of 303 GISTs (9.9%) were weak or negative for KIT and were analyzed in this study. All 30 GISTs consisted of epithelioid tumor cells exclusively or focally, although epithelioid GISTs are seen in about 20%-30% of all GISTs in general.[1,5,21] Of 273 KIT-positive GISTs in our cases, 226 (83%) GISTs were shown to be the spindle cell type, 38 (14%) were shown to be the mixed (combination of spindle and epithelioid cell) type, and 9 (3%) were shown to be the epithelioid cell type (data not shown). Histologically, we noticed different patterns within the epithelioid tumor cells in KIT-weak or KIT-negative GISTs. In some epithelioid GISTs, tumor cells arranged themselves in tightly cohesive patterns. In others, tumor cells loosely arranged themselves and were accompanied by myxoid stroma. We called the latter type of GISTs *myxoid epithelioid GISTs* in our study. Interestingly, subsequent mutational analyses showed a close relationship between these histological patterns and the type of mutations. Myxoid epithelioid GISTs closely correlated with *PDGFRA* gene mutations in both exons 12 and 18.

The *PDGFRA* gene mutations were found in 20 of the 30 KIT-weak or KIT-negative GISTs (66.6%). This rate is higher than that reported by Heinrich et al,[14] in whose study *PDGFRA* gene mutations were found in about 35% of GISTs without *c-kit* gene mutations. The rate became much higher when the cases were limited to the 20 myxoid epithelioid GISTs, of which 18 (90%) had *PDGFRA* gene mutations.

On the other hand, of 273 KIT-positive GISTs, 11 tumors were also accompanied by myxoid stroma, and 3 of those were of the epithelioid cell type resembling histology of myxoid epithelioid GISTs in this study. However, those 3 cases had mutations in the *c-kit* gene exon 11 but not in the *PDGFRA* gene (data not shown). Thus, the histology of myxoid epithelioid pattern in

KIT-weak or KIT-negative GISTs is considerably specific to GISTs with *PDGFRA* gene mutations. In only 2 GISTs with *PDGFRA* gene mutations (cases 17 and 29) were the GISTs not myxoid epithelioid. The tumor in case 17 was large and classified as high risk. Tumor progression may have influenced the morphology and growth pattern of the tumor cells in this case, although the tumor in case 29 was relatively small and was classified as low risk. In cases 6 and 12, *PDGFRA* gene mutations were not identified despite having a myxoid epithelioid pattern. However, the c-*kit* gene mutations were also not present in these cases. Mutations in other exons of the *PDFFRA* gene that we did not examine in this study might be present in these 2 tumors. Furthermore, we also found close relationships between myxoid epithelioid GISTs or GISTs with *PDGFRA* gene mutations and mast cell infiltration. In general, we frequently found mast cell infiltrations in various degrees in leiomyomas and leiomyosarcomas in the gastrointestinal tract and uterus.[22,23] Previous reports indicated that the numbers of mast cells within and around tumor nodules were thought to be a useful prognostic factor for soft tissue sarcomas.[23-25] In contrast, infiltrations of mast cells were observed in none of the KIT-positive GISTs with c-*kit* gene mutations in this study. We have used this histological difference for distinguishing between GISTs and other soft tissue tumors for some time. However, mast cell infiltration was observed in 18 of 30 GISTs (60%) in this study. Of these, 17 tumors were myxoid epithelioid GISTs (17 of 20, 85%). There is a close correlation between mast cell infiltrations and myxoid epithelioid patterns or *PDGFRA* gene mutations in GISTs ($P < 0.0001$). Very recently, Debiec-Rychter et al[26] also reported *PDGFRA* gene mutations in 3 (43%) of 7 KIT-negative GISTs, whereas their remaining tumors had no mutation in either c-*kit* or *PDGFRA* genes. In their reports, mast cell infiltrations were also seen within tumor nodule. Incidentally, mast cell infiltrations were not observed in 2 of 3 KIT-positive tumors resembling myxoid epithelioid GISTs in this study (data not shown).

At present, we have no evidence that explains the presence or absence of mast cell infiltrations among different types of GISTs. Stem cell factor (SCF), a natural ligand of the KIT receptor, is thought to be produced by smooth muscle cells and neurons in the gastrointestinal tract.[27,28] Mast cell infiltrations within leiomyomas and leiomyosarcomas are probably caused by SCF production by tumor cells that are of smooth muscle cell origin. On the other hand, SCF expression by tumor cells of GISTs has not been reported until now. However, we confirmed mRNA expression of both membrane-bound and soluble isoforms of SCF in all the KIT-positive GISTs by reverse-transcription PCR (data not shown). Rapid internalization of SCF by the SCF–KIT juxtacrine loop between tightly cohesive tumor cells may prevent mast cell infiltration in KIT-positive GISTs but not in myxoid epithelioid GISTs, which are less cohesive and weak or negative for KIT. Further studies about SCF expression in KIT-positive and KIT-weak or KIT-negative GISTs will be needed to explain the mechanism of mast cell infiltration in myxoid epithelioid GISTs.

GISTs are thought to originate from the ICCs because of the phenotypic similarity of specific molecules such as KIT, CD34, Smemb, and nestin.[8-12] However, in the human small intestine, a slow wave is also detected at the deep muscular plexus level, where KIT-positive ICCs are not present.[29] We previously observed KIT-negative, CD34-positive, ICC-like cells adjacent to KIT-positive ICCs in the stomach and small intestine.[11] The existence of KIT-negative fibroblast-like cells adjacent to KIT-positive ICCs has been reported.[30,31] GISTs with *PDGFRA* gene mutations may originate from such KIT-negative ICCs or other unknown mesenchymal cells, and that may reflect differences of histology and KIT expression. Further search and classification of ICCs and related mesenchymal cells and analysis of *PDGFRA* expression in such mesenchymal cells will be needed to confirm this hypothesis.

Although none of the patients with GISTs containing *PDGFRA* mutations died of disease, follow-up periods in this study are too short to conclude benign behavior of GISTs with *PDGFRA* mutations. Five of the 20 GISTs with the *PDGFRA* gene mutations were classified as high risk, and 1 of those (case 17) was treated with imatinib mesylate because of the residual tumor in the omentum. At present, the patient remains in partial remission. In this case, the mutation was deletion DIMH842-845 in exon 18 of the *PDGFRA* gene, and GISTs with this type of mutation have been reported to be sensitive to treatment with imatinib mesylate.[20] Mutational analysis and molecular subclassification of GISTs are now more important since the introduction of imatinib mesylate, because clinical responses to the drug and prognosis of patients are different in GISTs with different mutations.[20] However, the time and costs involved in analyzing all mutational hot spots in the c-*kit* and *PDGFRA* genes in GISTs present a problem for routine pathologic diagnosis. The results of this study suggest that it is best to analyze mutations in the *PDGFRA* gene first in myxoid epithelioid GISTs with mast cell infiltrations.

In conclusion, we analyzed 30 GISTs that were weak or negative for KIT in this study. We discovered a close correlation between a specific histological type of GISTs, myxoid epithelioid GISTs, and *PDGFRA* gene mutations. Myxoid epithelioid GISTs were accompanied by mast cell infiltrations that were not found in other types of GISTs. These histological characteristics may be useful for subsequent mutational analysis and molecular subclassification of GISTs.

REFERENCES

1. Mazur MT, Clark HB: Gastric stromal tumors: Reappraisal of histogenesis. Am J Surg Pathol 7:507-519, 1983

2. Ueyama T, Guo KJ, Hashimoto H, et al: A clinicopathologic and immunohistochemical study of gastrointestinal stromal tumors. Cancer 69:947-955, 1992

3. Franquemont DW, Frierson HF Jr: Muscle differentiation and

clinicopathological features of gastrointestinal stromal tumors. Am J Surg Pathol 16:947-954, 1992

4. Fletcher CD, Berman JJ, Corless C, et al: Diagnosis of gastrointestinal stromal tumors: A consensus approach. Hum Pathol 33: 459-465, 2002

5. Miettinen M, Lasota J: Gastrointestinal stromal tumors—definition, clinical, histological, immunohistochemical, and molecular genetic features and differential diagnosis. Virchows Arch 438:1-12. 2001

6. Ward SM, Burns AJ, Torihashi S, et al: Mutation of the proto-oncogene c-kit blocks development of interstitial cells and electrical rhythmicity in murine intestine. J Physiol 480:91-97, 1994

7. Burns AJ, Lomax AE, Torihashi S, et al: Interstitial cells of Cajal mediate inhibitory neurotransmission in the stomach. Proc Natl Acad Sci U S A 93:12008-12013, 1996

8. Hirota S, Isozaki K, Yasuhiro M, et al: Gain-of-function mutations of c-kit in human gastrointestinal stromal tumors. Science 279: 577-580, 1998

9. Sarlomo-Rikala M, Kovatich AJ, et al: CD117: A sensitive marker for gastrointestinal stromal tumors that is more specific than CD34. Mod Pathol 11:728-734, 1998

10. Kindblom LG, Remotti HE, Aldenborg F, et al: Gastrointestinal pacemaker cell tumor (GIPACT): Gastrointestinal stromal tumors show phenotypic characteristics of the interstitial cells of Cajal. Am J Pathol 152:1259-1269, 1998

11. Sakurai S, Fukasawa T, Chong JM, et al: Embryonic form of smooth muscle myosin heavy chain (SMemb/MHC-B) in gastrointestinal stromal tumor and interstitial cells of Cajal. Am J Pathol 154: 23-28, 1999

12. Tsujimura T, Makiishi-Shimobayashi C, Lundkvist J, et al: Expression of the intermediate filament nestin in gastrointestinal stromal tumors and interstitial cells of Cajal. Am J Pathol 158:817-823, 2001

13. Rubin BP, Singer S, Tsao C, et al: KIT activation is a ubiquitous feature of gastrointestinal stromal tumors. Cancer Res 61:8118-8121, 2001

14. Heinrich MC, Corless CL, Duensing A, et al: PDGFRA activating mutations in gastrointestinal stromal tumors. Science 299:708-710, 2003

15. Hirota S, Ohashi A, Nishida T, et al: Gain-of-function mutations of platelet-derived growth factor receptor alpha gene in gastrointestinal stromal tumors. Gastroenterology 125:660-667, 2003

16. Wardelmann E, Neidt I, Bierhoff E, et al: c-kit mutations in gastrointestinal stromal tumors occur preferentially in the spindle rather than in the epithelioid cell variant. Mod Pathol 15:125-136, 2002

17. Hasegawa T, Matsuno Y, Shimoda T, et al: Gastrointestinal stromal tumor: Consistent CD117 immunostaining for diagnosis, and prognostic classification based on tumor size and MIB-1 grade. Hum Pathol 33:669-676, 2002

18. van Oosterom AT, Judson I, Verweij J, et al: Safety and efficacy of imatinib (STI571) in metastatic gastrointestinal stromal tumors: A phase I study. Lancet 358:1421-1423, 2001

19. Demetri GD, von Mehren M, Blanke CD, et al: Efficacy and safety of imatinib mesylate in advanced gastrointestinal stromal tumors. N Engl J Med 347:472-480, 2002

20. Heinrich MC, Corless CL, Demetri GD, et al: Kinase mutations and imatinib response in patients with metastatic gastrointestinal stromal tumor. J Clin Oncol 21:4342-4349, 2003

21. Miettinen M, Sarlomo-Rikala M, Lasota J: Gastrointestinal stromal tumors: Recent advances in understanding of their biology. Hum Pathol 30:1213-1220, 1999

22. Maluf HM, Gersell DJ: Uterine leiomyomas with high content of mast cells. Arch Pathol Lab Med 118:712-714, 1994

23. Yavuz E, Gulluoglu MG, Akbas N, et al: The values of intratumoral mast cell count and Ki-67 immunoreactivity index in differential diagnosis of uterine smooth muscle neoplasms. Pathol Int 51:938-941, 2001

24. Ueda T, Aozasa K, Tsujimoto M, et al: Prognostic significance of mast cells in soft tissue sarcoma. Cancer 62:2416-2419, 1988

25. Tomita Y, Aozasa K, Myoui A, et al: Histologic grading in soft-tissue sarcomas. An analysis of 194 cases including AgNOR count and mast-cell count. Int J Cancer 54:194-199, 1993

26. Debiec-Rychter M, Wasag B, Stul M, et al: Gastrointestinal stromal tumors (GISTs) negative for KIT (CD 117 antigen) immunoreactivity. J Pathol 202:430-438, 2004

27. Ward SM, Ordog T, Bayguinov JR, et al: Development of interstitial cells of Cajal and pacemaking in mice lacking enteric nerves. Gastroenterology 117:584-594, 1999

28. Wu JJ, Rothman TP, Gershon MD: Development of the interstitial cell of Cajal: Origin, Kit dependence and neuronal and nonneuronal sources of Kit ligand. J Neurosci Res 59:384-401, 2000

29. Torihashi S, Horisawa M, Watanabe Y: c-kit immunoreactive interstitial cells in the human gastrointestinal tract. J Auton Nerv Syst 75:38-50, 1999

30. Vanderwinden JM, Rumessen JJ, de Kerchove d'Exaerde A Jr, et al: Kit-negative fibroblast-like cells expressing SK3, a Ca2+-activated K+ channel, in the gut musculature in health and disease. Cell Tissue Res 310:349-358, 2002

31. Fujita A, Takeuchi T, Jun H, Hata F: Localization of Ca2+-activated K+ channel, SK3, in fibroblast-like cells forming gap junctions with smooth muscle cells in the mouse small intestine. J Pharmacol Sci 92:35-42, 2003

Bioelectromagnetics 25:599–606 (2004)

Large Scale In Vitro Experiment System for 2 GHz Exposure

Takahiro Iyama,[1]* Hidetoshi Ebara,[1] Yoshiaki Tarusawa,[1] Shinji Uebayashi,[1] Masaru Sekijima,[2] Toshio Nojima,[3] and Junji Miyakoshi[4]

[1]Wireless Laboratories, NTT DoCoMo, Inc., Yokosuka, Japan
[2]Research Division for Advanced Technology, Kashima Laboratory, Mitsubishi Chemical Safety Institute Ltd., Kashima, Japan
[3]Division of Media and Network Technologies, Graduate School of Information Science and Technology, Hokkaido University, Hokkaido, Japan
[4]Department of Radiological Technology, School of Health Sciences, Faculty of Medicine, Hirosaki University, Hirosaki, Japan

A beam formed radiofrequency (RF) exposure-incubator employing a horn antenna, a dielectric lens, and a culture case in an anechoic chamber is developed for large scale in vitro studies. The combination of an open type RF exposure source and a culture case through which RF is transmitted realizes a uniform electric field (±1.5 dB) in a 300 × 300 mm area that accommodates 49 35 mm diameter culture dishes. This large culture dish area enables simultaneous RF exposure of a large number of cells or various cell lines. The RF exposure source operates at 2142.5 MHz corresponding to the middle frequency of the downlink band of the International Mobile Telecommunication 2000 (IMT-2000) cellular system. The dielectric lens, which has a gain of 7 dB, focuses RF energy in the direction of the culture case and provides a uniform electric field. The culture case is sealed and connected to the main unit for environmental control, located outside the anechoic chamber, via ducts. The temperature at the center of the tray, which contains the culture dishes in the culture room, is maintained at 37.0 ± 0.2 °C by air circulation. In addition, the appropriate CO_2 density and humidity supplied to the culture case realizes stable long term culture conditions. Specific absorption rate (SAR) dosimetry is performed using an electric field measurement technique and the Finite Difference Time Domain (FDTD) calculation method. The results indicate that the mean SAR of the culture fluid at the bottom of the 49 (7 × 7 array) culture dishes used in the in vitro experiments is 0.175 W/kg for an antenna input power of 1 W and the standard deviation of the SAR distribution is 59%. When only 25 culture dishes (5 × 5 array) are evaluated, the mean SAR is 0.139 W/kg for the same antenna input power and the standard deviation of the SAR distribution is 47%. The proliferation of the H4 cell line in 72 h in a pair of RF exposure-incubators reveals that the culture conditions are equivalent to those of a common CO_2 incubator. Bioelectromagnetics 25:599–606, 2004.

Key words: radiofrequency; SAR; dosimetry; in vitro; temperature regulation

INTRODUCTION

With the widespread use of mobile radio communication systems, many in vitro studies related to radiofrequency (RF) exposure have been conducted. In general, such studies require experimental systems that provide the RF exposure of the cells as well as the stability of the CO_2 density, humidity conditions, and temperature regulation surrounding the cells.

Several kinds of RF exposure systems have been reported for in vitro studies so far. These systems comprise an RF exposure source and an environmental control unit, and they fall into two categories: closed and open types. In the closed type, the RF exposure source is often placed in a common environmental control unit called a CO_2 incubator. In the open type, the environmental control unit is usually self-contained and the RF exposure source is located separately.

For closed type RF exposure systems, the use of a transverse electromagnetic (TEM) cell [Burkhardt et al., 1996], a rectangular waveguide [Schönborn et al., 2000] and a wire patch cell [Laval et al., 2000]

*Correspondence to: Takahiro Iyama, Wireless Laboratories, NTT DoCoMo, Inc., 3-5, Hikari-no-oka, Yokosuka, Kanagawa, 239-8536, Japan. E-mail: iyama@mlab.yrp.nttdocomo.co.jp

Received for review 11 June 2003; Final revision received 26 March 2004

DOI 10.1002/bem.20038
Published online in Wiley InterScience (www.interscience.wiley.com).